

Genetic identification and characterization of chromosomal regions for kernel length and width increase from tetraploid wheat

Jieguang Zhou

Sichuan Agricultural University

Cong Li

Sichuan Agricultural University

Jianing You

Sichuan Agricultural University

Huaping Tang

Sichuan Agricultural University

Yang Mu

Sichuan Agricultural University

Qiantao Jiang

Sichuan Agricultural University

Yaxi Liu

Sichuan Agricultural University

Guoyue Chen

Sichuan Agricultural University

Jirui Wang

Sichuan Agricultural University

Pengfei Qi

Sichuan Agricultural University

Jun Ma

China Agricultural University

Yutian Gao

China Agricultural University

Ahsan Habib

Khulna University

Yuming Wei

Sichuan Agricultural University

Youliang Zheng

Sichuan Agricultural University

Xiujin Lan

Sichuan Agricultural University

Jian Ma (✉ jianma@sicau.edu.cn)

Sichuan Agricultural University

Keywords: Tetraploid wheat, Wheat 55K SNP array, Kernel size, QTL validation,

Posted Date: April 26th, 2021

DOI: <https://doi.org/10.21203/rs.3.rs-397027/v1>

License:   This work is licensed under a Creative Commons Attribution 4.0 International License. [Read Full License](#)

Abstract

Background: Improvement of wheat (*Triticum aestivum* L.) yield could relieve global food shortages. Kernel size, as an important component of 1000-kernel weight (TKW), is always a significant consideration to improve yield for wheat breeders. Wheat related species possesses numerous elite genes that can be introduced into wheat breeding. It is thus vital to explore, identify, and introduce new genetic resources for kernel size from wheat wild relatives to increase wheat yield.

Results: In the present study, quantitative trait loci (QTL) for kernel length (KL) and width (KW) were detected in a recombinant inbred line (RIL) population derived from a cross between a wild emmer accession 'LM001' and a Sichuan endemic tetraploid wheat 'Ailanmai' using the Wheat 55K single nucleotide polymorphism (SNP) array-based constructed linkage map and phenotype from six different environments. We identified eleven QTL for KL and KW including two major ones *QKL.sicau-AM-3B* and *QKW.sicau-AM-4B*, the positive alleles of which were from LM001 and Ailanmai, respectively. They explained 17.57% to 44.28% and 13.91% to 39.01% of the phenotypic variance, respectively. For these two major QTL, Kompetitive allele-specific PCR (KASP) markers were developed and used to successfully validate their effects in three F₃ populations and two natural populations containing a panel of 272 Chinese wheat landraces and that of 300 Chinese wheat cultivars, respectively. *QKL.sicau-AM-3B* was located at 666.2-685.9 Mb on chromosome arm 3BL. *QKW.sicau-AM-4B* was located at 639.7-696.4 Mb on chromosome arm 4BL. Comparison with previous studies suggested that these two major QTL were likely new loci. Further analysis indicated that the positive alleles of *QKL.sicau-AM-3B* and *QKW.sicau-AM-4B* had a great additive effect increasing TKW by 6.40%. Correlation analysis between KL and other agronomic traits showed that KL was significantly correlated to spike length, length of uppermost internode, TKW, and flag leaf length. KW was also significantly correlated with TKW. Four genes, *TRIDC3BG062390*, *TRIDC3BG062400*, *TRIDC4BG037810*, and *TRIDC4BG037830*, associated with kernel development were predicted in physical intervals harboring these two major QTL on wild emmer and Chinese Spring reference genomes.

Conclusions: Two stable and major QTL for KL and KW across six environments were detected and verified in three biparental populations and two natural populations. Significant relationships between kernel size and yield-related traits were identified. KASP markers tightly linked the two major QTL could contribute greatly to subsequent fine mapping. These results suggested the application potential of wheat related species in wheat genetic improvement.

Background

Wheat (*Triticum aestivum* L.) is one of the main food crops in the world [1]. The pace of population growth requires a stable increase of wheat yield [2]. Wheat yield is determined by three key components, including productive spike number per unit area, kernel number per spike, and 1000-kernel weight (TKW) [3]. TKW is mainly affected by kernel size including kernel length (KL), kernel width (KW), and kernel thickness [4]. Therefore, KL and KW play vital roles in wheat yield formation.

To date, quantitative trait loci (QTL) for kernel size have been detected on all of the wheat chromosomes [5]. For example, seven QTL for KW were detected on chromosomes 1A, 4D, 5A, 5B, 6D, and 7B [6]. Three stable QTL were identified in more than three environments, including two for KL and one for KW [7]. Xin et al. [8] identified two QTL for KW. Furthermore, several genes for kernel size have been isolated and cloned in wheat via a map-based cloning approach. For example, the grain-shape gene *Tasg-D1* encoding a Ser/Thr protein kinase glycogen synthase kinase3 was associated with formation of round grains in wheat [9]. *Keto-acyl thiolase 2B* (*KAT-2B*) involved in β -oxidation during JA synthesis played a role in determination of kernel weight [10].

Wheat breeding is facing the bottleneck of narrow genetic basis at present [11]. Fortunately, a large diversity of undeveloped genetic resources from wheat related species could contribute to meeting future wheat production

challenges. It is feasible to identify and utilize novel QTL/genes for KL and KW from excellent germplasms of wheat and its related species [12]. For example, a major QTL (*QGD-4BL*) controlling kernel size of the upper spikelet was identified in wild emmer (*T. turgidum* ssp. *dicoccoides*) [13]. Four QTL for KL and one for KW were detected in durum wheat [14]. Okamoto et al. [15] found that *P1* had a positive effect on KL in Polish wheat (*T. turgidum* ssp. *polonicum*). *TtGRF4-A* (ortholog of rice *OsGRF4*) was associated with kernel size and kernel weight in wild emmer [16].

As the progenitor of modern tetraploid and hexaploid cultivated wheat, wild emmer has the highest nucleotide diversity across the *Triticum* taxonomic groups making it an invaluable gene pool for the genetic improvement of wheat [17]. Thus, identification of QTL/genes for KL and KW from wild emmer will facilitate progress to meet wheat production challenges in the future. In this study, we are aiming at identifying and validating major QTL for KL and KW in a recombinant inbred line (RIL) population derived from a cross between a wild emmer accession and a Sichuan endemic tetraploid wheat 'Ailanmai'.

Materials And Methods

Genetic populations

Four bi-parent populations developed by the single-seed descent method were used in this study. They were derived from crosses Ailanmai × LM001 (AM, 121 F₈ RILs including parents) [18], LM001 × PI 503554 (MP, 102 F₃ lines), Ailanmai × AS 2268 (AAs, 102 F₃ lines), and Ailanmai × PI 193877 (API, 72 F₃ lines). Notably, the 121 RILs of AM were previously genotyped using the Wheat 55K SNP array [18] and used for QTL mapping in this study. The other three populations were used for validating QTL identified in this study. Ailanmai (*T. turgidum* L. $2n = 4x = 28$, AABB) is a local dwarf variety from Sichuan province, and LM001 is a wild emmer accession (*T. turgidum* ssp. *dicoccoides*, $2n = 4x = 28$, AABB). PI 503554 (*T. turgidum* ssp. *durum*) and PI 193877 (*T. turgidum* ssp. *dicoccon*) were from The U.S. National Plant Germplasm System (NPGS), and AS 2268 (*T. carthlicum* Nevski) was collected and preserved by Triticeae Research Institute of Sichuan Agricultural University. Besides, two natural populations were further used to verify the effect of the major QTL, and they were: (I) a panel of 272 Chinese wheat landraces (CWL) genotyped using the Wheat 660K SNP array [19], and (II) a panel of 300 Chinese wheat cultivars (CWC) genotyped using the Wheat 55K SNP array [20]. The information of two natural populations was listed in Table S1.

Phenotypic Evaluation

The phenotype of AM RIL population was measured in six different environments, including Chongzhou (103°38'E, 30°32'N) in 2017, 2018, 2019, and 2020 (2017CZ, 2018CZ, 2019CZ, and 2020CZ), Wenjiang (103°51'E, 30°43'N) in 2020 (2020WJ), and Ya'an (103°0'E, 29°58'N) in 2020 (2020YA) in China. All trials were performed in a randomized block design with two replications. Each line was single-seed planted in one row of 1.5 meters in length with 0.1 meters between plants within a row and 0.3 meters between rows. Field management was according to local agricultural practices [21]. Thirty kernels in each line were scanned using Epson Expression 10,000 XL. KL and KW were evaluated using WinSEEDLE (Regent Instruments Canada Inc) based on the selected objects in image [21]. Then, the average values were used for QTL detection and further analysis. The data of spike length (SL), effective tiller number (ETN), length of uppermost internode (UIL), TKW, and grain number per spike (GNS) were retrieved from our previous study [18]. The measurement of flag leaf length (FLL) and flag leaf width (FLW) was conducted about ten days after anthesis. The FLL (from leaf bottom to the tip) and FLW (on the widest part of the leaf) were measured on five selected plants (five typical plants per row for each line) from the main tiller of each plant [22]. Details of environmental information of agronomic traits measurement were listed in Table S2.

The 272 CWL were planted in six different environments, including 2012YA, 2013-2015WJ, and 2014-2015CZ [19]. The mean value of each accession in a single environment was used for further analysis [19].

The 300 CWC were planted in three different environments, including Beijing in 2018 and 2019, and Baoding in 2019 [20]. One hundred and twenty seeds of each accession were planted in a single row of 2 meters in length with 0.7 meters spacing between the rows in three environments [20]. The kernel-related traits were measured using the SC-G wheat grain appearance quality image analysis system developed by the Hangzhou WSeen Detection Technology Co [20].

Data analysis

SAS 8.0 (SAS Institute, Cary, NC, USA) was used to analyze the best linear unbiased prediction (BLUP) of the agronomic traits and the broad-sense heritability (H^2) in different environments. According to the description of Smith et al. [23], the SPSS Statistic 24.0 program (IBM SPSS, Armonk, NY, USA) was used to obtain Pearson's correlation coefficients within agronomic traits based on the BLUP values, descriptive statistical analyses, and independent sample t -test ($P < 0.05$). Frequency distributions of KL and KW values were plotted in the Origin 9.0 software using Gaussian distribution. Furthermore, the individuals of the AM RILs were divided into two groups based on the genotypes of the closest markers for each of the two major QTL, and then the differences between the two groups for the corresponding traits were analyzed.

QTL Mapping

High-quality genomic DNA was extracted from young leaves of AM RIL plants using the Plant Genomic DNA Kit (Tiangen Biotech, Beijing, China). The qualified DNA of each line was genotyped using the wheat 55K SNP array at CapitalBio Technology company (Beijing, China). The genetic map was constructed by Mo et al. [18].

The inclusive composite interval mapping (ICIM) in IciMapping 4.1 (<https://www.isbreeding.net/>) was used to detect QTL, and thousand permutations test ($p < 0.05$) was used for defining QTL logarithm (base 10) of odds scores (LOD) threshold [24]. A LOD score of 2.5 was chosen as a threshold for considering significant QTL [25]. The QTL \times Environment (QE) interaction effects were analyzed using IciMapping with the preset parameter: step = 1 cM, PIN = 0.001, LOD = 5.0. In the present study, QTL identified in more than three environments and expressed more than 10% of the phenotype variance explained (PVE) were defined to be major ones, and those with less than 1 cM apart were treated as an identical one [26]. Furthermore, QTL were named in accordance with the International rules of Genetic Nomenclature (<http://wheat.pw.usda.gov/ggpages/wgc/98/Intro.htm>). The 'sicaui' represents Sichuan Agricultural University.

Marker Development And QTL Validation

Two SNP markers were converted to Kompetitive allele-specific PCR (KASP) markers as previously described [26]. The KASP marker, *KASP-AX-111112626* (Table S3), tightly linked to *QKL.sicaui-AM-3B*, was used to verify the effect of *QKL.sicaui-AM-3B* in MP population. While *KASP-AX-108974756* (Table S3) was used to validate the effect of *QKW.sicaui-AM-4B* in two populations (AAs and API) with different genetic backgrounds.

Firstly, we selected 102, 72, and 102 lines from the AAs, API, and MP populations, respectively, and then divided the homozygous lines into two groups (Data set 1 and 2) based on the genotyping results. Data set 1 represented lines with homozygous alleles from Ailanmai or LM001, whereas Data set 2 represented lines with homozygous alleles from the other parents. Finally, we evaluated the differences in KL or KW between the two groups with the independent sample t -test ($P < 0.05$) to determine the effects of the major QTL.

The flanking marker *AX-111112626* was included in CWL natural population genotyped using the Wheat 55K SNP array and *AX-108974756* was included in the CWC natural population genotyped using Wheat 660K SNP array. The genotypes selected based on genotype of these two flanking makers were also divided into two groups in each population. The BLUP values of KL and KW data from all environments of CWL and CWC were used to analyze the differences with the independent sample t -test ($P < 0.05$) between the two groups.

Physical intervals of the major QTL and comparison with previously reported QTL

In order to predicate physical intervals of the major QTL identified in this study, the sequences of their flanking markers were used to blast against (E -value of $1e-5$) genomes sequences of the wild emmer (<https://www.dropbox.com/sh/3dm05grokhl0nbv/AAC3wvIYmAher8fY0srX3gX9a?dl=0%22>) [27] and the International Wheat Genome Sequencing Consortium (IWGSC) Chinese Spring (CS) RefSeq v1.0 (<https://urgi.versailles.inra.fr/download/iwgs/>) [28]. The annotations and functions of genes were retrieved on UniProt (<http://www.uniprot.org/>). We compared physical distances by anchoring flanking marker sequences of KL and KW QTL obtained in previous studies on CS to indicate whether the currently determined QTL were novel.

Furthermore, to identify the possible regulatory genes of KL and KW, the spatio-temporal expression patterns of the genes that were identified in the intervals of *QKL.sicau-AM-3B* and *QKW.sicau-AM-4B* were analyzed using the Triticeae Multi-omics Center website (<https://202.194.139.32/expression/index.html>). For *TraesCS4B01G212200* and *TraesCS4B01G212300*, their spatio-temporal expression patterns were analyzed using Chinese Spring cv-1 Development (single) on the Triticeae Multi-omics Center website (<https://202.194.139.32/expression/index.html>).

Results

Phenotypic data analyses

LM001 showed longer and narrower kernel than Ailanmai (Fig. 1; Table 1). The values of the KL and KW in each environment showed a continuous distribution (Fig. S1a, b). The KL and KW ranged from 5.86 to 9.43 mm and from 2.74 to 4.16 mm, respectively, in the AM RIL population (Table 1). The standard deviation (STD) of KL and KW ranged from 0.45 to 0.60 and from 0.11 to 0.24, respectively. H^2 of KL and KW were 0.79 and 0.72, respectively (Table 1). The result indicated that both KL and KW had high repeatability over testing environments, suggesting KL and KW were mainly controlled by genetic factors.

Table 1

Phenotype variance explained (PVE), standard deviation (STD) and the broad-sense heritability (H^2) of kernel length (KL) and width (KW) for the parents and AM RIL population in different environments.

Trait	Environment	Parents		Ailanmai × LM001 (AM)			
		Ailanmai	LM001	Range	Mean	STD	H^2
KL (mm)	2017CZ	N	N	5.96–9.06	8.11	0.56	0.79
	2018CZ	6.28**	8.15	5.90–9.00	8.14	0.58	
	2019CZ	6.67**	8.65	6.59–9.40	8.46	0.52	
	2020CZ	6.28**	8.35	6.51–9.43	8.48	0.54	
	2020WJ	6.56**	8.49	5.86–9.16	8.25	0.60	
	2020YA	6.70**	8.52	7.18–9.11	8.46	0.45	
	BLUP	6.58**	8.39	6.47–9.04	8.31	0.46	
	KW (mm)	2017CZ	N	N	2.89–3.72	3.43	0.19
2018CZ		3.90**	3.34	3.16–3.82	3.54	0.15	
2019CZ		3.92**	3.42	3.21–4.16	3.64	0.20	
2020CZ		3.96**	3.35	2.74–3.95	3.49	0.24	
2020WJ		3.91**	3.33	3.19–4.14	3.58	0.18	
2020YA		3.81**	3.37	2.92–3.87	3.46	0.20	
BLUP		3.82**	3.38	3.26–3.80	3.52	0.11	

KL: kernel length; KW: kernel width; CZ: Chongzhou; WJ: Wenjiang; YA: Ya'an; STD: standard deviation; H^2 : the broad-sense heritability; BLUP: phenotype values based on BLUP; N: the data was missing; ** Significance at the 0.01 probability level; * Significance at the 0.05 probability level.

Correlation Analyses Between Kernel Traits And Other Yield-related Traits

Significant and positive correlations for KL and KW were detected in most different environments ($P < 0.05$). The correlation coefficients ranged from 0.62 to 0.82 for KL and from 0.29 to 0.45 for KW, respectively (Table 2).

Table 2
Correlation coefficients of KL and KW in different environments.

Trait	Environment	2017CZ	2018CZ	2019CZ	2020CZ	2020WJ	2020YA
KL	2017CZ	1					
	2018CZ	0.72**	1				
	2019CZ	0.67**	0.82**	1			
	2020CZ	0.62**	0.70**	0.77**	1		
	2020WJ	0.65**	0.71**	0.81**	0.69**	1	
	2020YA	0.76**	0.79**	0.80**	0.72**	0.75**	1
KW	2017CZ	1					
	2018CZ	0.33**	1				
	2019CZ	0.45**	0.12	1			
	2020CZ	0.43**	0.29**	0.36**	1		
	2020WJ	0.26	0.33**	0.33**	0.45**	1	
	2020YA	0.43**	0.29**	0.36**	0.37**	0.29**	1
KL: kernel length; KW: kernel width; CZ: Chongzhou; WJ: Wenjiang; YA: Ya'an; ** Significance at the 0.01 probability level; * Significance at the 0.05 probability level.							

The BLUP datasets of kernel size and yield-related traits were employed to evaluate their relationships. Correlation analysis showed that significant correlations ($P < 0.05$) were observed between KL and SL, UIL, TKW, FLL ($r = 0.28$ to 0.66 ; Fig. S2a, c, d, and g). However, there were no significant correlations between KL and ETN, GNS, KW, FLW ($r = -0.061$ to 0.10 ; Fig. S2b, e, f, and h). Moreover, KW showed significant correlations ($P < 0.05$) with TKW ($r = 0.31$; Fig. S2i), but the other six agronomic traits (SL, ETN, UIL, GNS, FLL and FLW) were not significantly correlated to the KW ($r = -0.16$ to 0.13 ; Fig. S2i, j, k, m, n, and o).

QTL Detection

A total of eleven putative QTL associated with KL (six QTL) and KW (five QTL) were identified in the AM population and they were located on chromosomes 1B, 2A, 2B, 3B, 4B, 6A, 6B, and 7A (Table 3).

Table 3
Quantitative trait loci (QTL) mapping for kernel length (KL) and kernel width (KW).

Trait	QTL	Environment	Chromosome	Left Marker	Right Marker	LOD	PVE (%)	Add	CI
KL	<i>QKL.sicau-AM-6A</i>	2019CZ	6A	AX-109843320	AX-108755285	2.55	4.56	-0.12	10.5–21.5
	<i>QKL.sicau-AM-2B</i>	2018CZ	2B	AX-108730087	AX-110447950	3.06	5.38	-0.20	21.5–37.5
	<i>QKL.sicau-AM-3B</i>	2018CZ	3B	AX-111112626	AX-110375013	4.22	17.57	-0.24	1.5–7.5
		2019CZ		AX-111112626	AX-110375013	15.84	44.28	-0.35	4.5–7.5
		2020CZ		AX-111112626	AX-110375013	12.45	37.50	-0.35	3.5–7.5
		2020WJ		AX-111112626	AX-110375013	7.69	27.70	-0.32	2.5–7.5
		2020YA		AX-111112626	AX-110375013	10.03	32.55	-0.26	2.5–7.5
		BLUP		AX-111112626	AX-110375013	11.58	34.55	-0.29	2.5–7.5
	<i>QKL.sicau-AM-3B.1</i>	2017CZ	3B	AX-108914590	AX-108727907	3.90	13.57	-0.21	10.5–13.5
	<i>QKL.sicau-AM-4B</i>	BLUP	4B	AX-109410422	AX-94486277	3.62	15.68	0.03	81.5–83.0
	<i>QKL.sicau-AM-6B</i>	2017CZ	6B	AX-109336882	AX-110062048	3.37	18.59	0.19	127.5–130.5
KW	<i>QKW.sicau-AM-2A</i>	BLUP	2A	AX-108949998	AX-109355803	3.38	22.96	0.03	134.5–140.5
	<i>QKW.sicau-AM-7A</i>	BLUP	7A	AX-108885515	AX-109302546	2.86	26.22	-0.03	91.5–97.5
	<i>QKW.sicau-AM-1B</i>	BLUP	1B	AX-111062860	AX-110067443	4.98	29.08	0.04	79.5–81.5
	<i>QKW.sicau-AM-2B</i>	2019CZ	2B	AX-109897880	AX-110598098	2.96	29.82	0.06	11.5–13.5
	<i>QKW.sicau-AM-4B</i>	2017CZ	4B	AX-108974756	AX-111451315	7.77	25.17	0.10	12.5–14.5
		2018CZ		AX-108974756	AX-111451315	10.10	38.44	0.09	12.5–14.5
		2019CZ		AX-108955591	AX-110915030	3.81	13.91	0.07	14.5–15.5
		2020CZ		AX-108955591	AX-110915030	8.91	29.97	0.13	14.5–15.5

KL: kernel length; KW: kernel width; CZ: Chongzhou; WJ: Wenjiang; YA: Ya'an; LOD: logarithmic odds; PVE: phenotype variation values. Add: additive effect of a QTL, positive values indicate that alleles from Ailanmai are increasing the trait scores, and negative values indicate that alleles from LM001 are increasing the trait scores. CI: confidence interval of the QTL.

Trait	QTL	Environment	Chromosome	Left Marker	Right Marker	LOD	PVE (%)	Add	CI
		2020WJ		AX-108955591	AX-110915030	5.98	23.31	0.08	14.5–15.5
		2020YA		AX-108955591	AX-110915030	5.58	24.02	0.09	14.5–15.5
		BLUP		AX-108955591	AX-110915030	18.17	39.01	0.08	14.5–15.5
KL: kernel length; KW: kernel width; CZ: Chongzhou; WJ: Wenjiang; YA: Ya'an; LOD: logarithmic odds; PVE: phenotype variation values. Add: additive effect of a QTL, positive values indicate that alleles from Ailanmai are increasing the trait scores, and negative values indicate that alleles from LM001 are increasing the trait scores. CI: confidence interval of the QTL.									

Six QTL for KL explained 4.56–44.28% of the PVE. *QKL.sicau-AM-3B*, a major and stable locus, was detected in five environments and BLUP data, and explained 17.57–44.28% of the PVE. The positive allele was from LM001 (Table 3). The remaining five QTL detected in a single or two environments explained between 4.56% and 18.59% of the PVE.

Furthermore, five QTL for KW explained 13.91–39.01% of the PVE. *QKW.sicau-AM-4B*, a major QTL, detected in all the six environments and also the BLUP data. This locus could explain 13.91–39.01% of the PVE, and the positive allele was contributed by Ailanmai (Table 3). The other four QTL were detected in less than three environments, and they explained between 22.96% and 29.82% of the PVE (Table 3). Furthermore, twenty-eight QTL were detected using QE interaction analysis (Table S4). *QKL.sicau-AM-3B* controlling KL and *QKW.sicau-AM-4B* controlling KW were simultaneously identified by multi-environmental and individual environmental analyses, further showing that they were major and stable QTL.

Verification Of The Major QTL In Different Genetic Backgrounds

A KASP marker, *KASP-AX-111112626*, tightly linked to *QKL.sicau-AM-3B* and one, *KASP-AX-108974756*, tightly linked to *QKW.sicau-AM-4B* were developed to validate their effects in different genetic backgrounds (Table S3; Fig. 2).

According to the polymorphism of *KASP-AX-111112626*, the lines were divided into two groups in the AM RIL population: lines with Ailanmai homozygous allele and lines with LM001 homozygous allele (excluding heterozygosis). The group with positive allele of *QKL.sicau-AM-3B* (from LM001) had significantly greater values than that with negative one (from Ailanmai) in each environment and BLUP data set ($P < 0.05$; Fig. 2a and b). Likewise, the lines from CWL population were divided into two groups. The group with positive allele of *QKL.sicau-AM-3B* had 3.29% higher values than that with negative one ($P < 0.05$; Fig. 3d). In MP population, the lines with positive allele had 11.46% higher values than those with negative one, indicating that *QKL.sicau-AM-3B* is indeed a major QTL controlling KL (Fig. 3a).

Additionally, according to the polymorphism of *KASP-AX-108974756*, the lines from AM population were also divided into two groups. The group with positive allele of *QKW.sicau-AM-4B* had significantly higher values than that with negative one in six environments and BLUP data set ($P < 0.05$; Fig. 2c, d). In CWC population, the group with positive allele of *QKW.sicau-AM-4B* had significantly 0.78% greater values than that with negative one ($P < 0.05$; Fig. 3e). In AAs and API populations, the group with positive allele from Ailanmai had significantly greater values than that without this allele, and the differences between the two groups were 10.17% and 10.08%, respectively, with an average of 10.13% in two validation populations, indicating that *QKW.sicau-AM-4B* is also a major QTL controlling KW (Fig. 3b, c).

Effects of *QKL.sicau-AM-3B* and *QKW.sicau-AM-4B* on TKW in AM population

In AM population, the positive alleles of *QKL.sicau-AM-3B* and *QKW.sicau-AM-4B* were from LM001 and Ailanmai, respectively (Table 3). The effects of *QKL.sicau-AM-3B* and *QKW.sicau-AM-4B* on TKW were further analyzed (Fig. 5). Compared with those without any of the alleles increasing KL and KW, lines possessed the positive allele of *QKL.sicau-AM-3B* but not that of *QKW.sicau-AM-4B* increased TKW by 2.82%; lines possessed that of *QKW.sicau-AM-4B* but not that of *QKL.sicau-AM-3B* increased TKW by 2.32%; and those with the combination of positive alleles of both *QKL.sicau-AM-3B* and *QKW.sicau-AM-4B* significantly increased TKW by up to 6.40% ($P < 0.05$). Besides, lines with the combination of positive alleles of *QKL.sicau-AM-3B* and *QKW.sicau-AM-4B* significantly increased TKW by 3.48% and 3.98% ($P < 0.05$), respectively, compared to those with the positive allele of the *QKL.sicau-AM-3B* only or the *QKW.sicau-AM-4B* only (Fig. 5).

Discussion

Relationship between kernel size and other agronomic traits

In this study, we evaluated the correlation coefficients between kernel size and other agronomic traits (Fig. S2). Positive and significant correlations were observed between KL, KW, and TKW ($P < 0.05$; Fig. S2d, l). The result indicated that the selection of larger kernels might lead to indirect selection of heavier kernels [29]. As expected, KL and KW were positively correlated with UIL (Fig. S2c, k). A longer UIL contributed to ventilation, light transmittance, and lower relative humidity of spikes, thus reducing the possibility of occurrence of diseases and insect pests such as scab, which was conducive to dry matter accumulation and affects kernel size [30]. KL and FLL showed significant positive correlation, and KW was positively correlated with FLW ($P < 0.05$; Fig. S2g, o). Theoretically, FLL and FLW determined the flag leaf area that was proportional to whether it had a strong assimilation tissue, vascular bundle area and these factors determined the kernel filling intensity of wheat, which was closely correlated with kernel size [31]. Furthermore, the results indicated that larger flag leaves increased yield by providing more photosynthetic nutrient to kernel [32]. The above conclusions provided a scientific basis for evaluating complex relationships among wheat yield components, which will be helpful in understanding increase of wheat yield.

Stable And Novel QTL Controlling KL And KW

We compared the major QTL identified in this study with those detected in previous studies through aligning physical positions of their closest markers (Table S5).

QKL.sicau-AM-3B was located between 666.2 and 685.9 Mb in the deletion bin 3BL7-0.63-1.00 on chromosome arm 3BL in wild emmer (Fig. 4a, c), which was different from previously reported KL-related QTL (Table S5). For example, *QGI-3B.1* was detected on chromosome arm 3BS at 52.1–53.2 Mb [33]. And *QGI.ccsu-3B.1* was flanked by marker *Xgwm376* (38.9 Mb) [34]. Two QTL, *QKL.ndsu.3B* and *QKL.ndsu.3B.1*, were located at 211.7-216.3 Mb and 233.9-244.6 Mb, respectively [35]. And *qKL.3B* was identified on chromosome arm 3BS with the closest marker *Xgwm429* (20.5 Mb) [36]. Thus, these results indicated *QKL.sicau-AM-3B* may be a novel QTL controlling KL detected in the present study.

For KW, *QKW.sicau-AM-4B* was located between 439.7 and 469.4 Mb in the deletion bin 4BL1-0.71 and 4BL1-0.71-0.86 on chromosome arm 4BL in wild emmer (Fig. 4e, g). Comparison of physical positions of *QKW.sicau-AM-4B* with those reported previously suggested that they were not overlapped (Table S5). For example, there were five QTL, *QKw.ncl-4B.1* [37], *QGw-4B.1* [33], *Size width 2011* [14], *QKw4B.1-7* [38], *QKw-4B.2* [39], and *kw-WY-4B-1.2* [40], associated with KW being detected on chromosome arm 4BS. *qKW-4B* was identified on chromosome arm 4BL with the closest marker *Xwmc657* (610.5 Mb) [36], and *qKW4B-1* was detected on chromosome arm 4BL at 610.1-649.1 Mb [8]. These results showed that *QKW.sicau-AM-4B* is probably a novel QTL controlling KW in wheat.

Predictive genes in the intervals where major QTL were located

QKL.sicau-AM-3B was located between 666.2 and 685.9 Mb on wild emmer 3BL and between 655.4 and 675.6 Mb on CS 3BL by anchoring flanking markers *AX-111112626* and *AX-110375013* of *QKL.sicau-AM-3B* (Fig. 4a, b, c, and d). There

were thirty-eight shared predicated genes (Table S6). Expression analyses showed that thirty-one genes can be expressed in kernel (Fig. S3a). Similarly, for *QKW.sicau-AM-4B*, it was mapped between 439.7 and 469.4 Mb on chromosome arm 4BL of wild emmer and 433.7 and 463.2 Mb on chromosome arm 4BL of CS by anchoring its flanking markers *AX-108974756* and *AX-110915030* (Fig. 4e, f, g and h). There were forty-seven shared predicated genes (Table S6). Expression analyses showed that forty-two genes can be expressed in kernel (Fig. S3b).

Of these eighty-five genes, four genes were involved in kernel development. For example, *TRIDC3BG062390* encoded fructose-bisphosphate aldolase (FBA) and it had a higher expression in kernel than other genes (Fig. S3a). FBA is an important isozyme involved in plant metabolism, and it is directly involved in the fixation and distribution of photosynthate [41]. Cytosolic and plastidic FBAs were expressed in plant photosynthetic tissues [42]. FBA regulates kernel size development through affecting plant photosynthesis. In addition, there were two un-functional and annotated genes of wild emmer, *TRIDC4BG037810* and *TRIDC4BG037830*. Nonetheless, they were highly expressed in kernel at different growth stages (Fig. S4a, b). Therefore, we identified annotations of their orthologs in CS [28]. *TraesCS4B01G212200* (*TRIDC4BG037810*) and *TraesCS4B01G212300* (*TRIDC4BG037830*) encoded Heat-shock protein (HSP; Table S6) and were also highly expressed in kernel (Fig. S4c, d). HSP was widely reported in graminaceous plant [43]. At high temperature, the role of HSP is to ensure the normal growth of kernel in wheat through providing protection to soluble starch synthase [44]. It was reported that HSP, as a molecular chaperone, aids in refolding soluble starch synthases denatured by heat and thus prevents them from aggregating, which was beneficial to starch synthesis of in kernel [45]. Thus, these genes related to kernel development may provide information for fine mapping and gene cloning of these identified major and novel QTL.

Utilization of elite alleles for kernel size from wheat related species

In the current study, two major, stably expressed, and novel QTL, *QKL.sicau-AM-3B* and *QKW.sicau-AM-4B* for kernel-related traits were identified from a wild emmer accession and a local landrace and validated in five populations with different genetic backgrounds. The combination of *QKL.sicau-AM-3B* and *QKW.sicau-AM-4B* had the largest additive effect on TKW (Fig. 5). These results suggest that they have a great potential in wheat breeding. Previous studies showed that pyramiding of choiceness genes was an effective method to improve a given trait [46]. In this study, we found some transgressive segregations in AM RIL. For example, AM-3 has longer and wider kernels than both parents (Fig. 1). Interestingly, AM-3 carries the positive alleles of both *QKL.sicau-AM-3B* and *QKW.sicau-AM-4B*, implying the possibility of pyramiding these two positive alleles from wheat related species in wheat breeding.

Conclusions

Two major and novel QTL, *QKL.sicau-AM-3B* and *QKW.sicau-AM-4B*, were identified in AM RIL population. Both of them were successfully verified in their corresponding validation populations with newly developed KASP makers. Some genes involved in regulation of kernel growth and development were detected in the intervals where major KL and KW QTL were located. Significant correlations between kernel size and other agronomic traits were detected and discussed. KASP markers tightly linked the two major QTL could contribute greatly to subsequent fine mapping. This study indicated that wheat related species have great potentials for wheat yield improvement.

Abbreviations

QTL: Quantitative trait loci; KL: Kernel length; KW: Kernel width; TKW: 1000-kernel weight; SL: Spike length; ETN: Effective tiller number; UIL: Length of uppermost internode; GNS: Grain number per spike; FLL: Flag leaf length; FLW: Flag leaf width; AM: Ailanmai × LM001; RILs: Recombinant inbred lines; PVE: Phenotypic variance explained; KASP: Kompetitive allele-specific PCR; SNP: Single-nucleotide polymorphism; MP: LM001 × PI 503554; AAs: Ailanmai × AS 2268; API: Ailanmai × PI 193877; NPGS: The U.S. National Plant Germplasm System; CWL: Chinese wheat landraces; CWC: Chinese

wheat cultivars; CZ: Chongzhou; WJ: Wenjiang; YA: Ya'an; BLUP: Best linear unbiased prediction; H^2 : Broad-sense heritability; LOD: Logarithm of odds; QE: QTL \times Environment; CS: Chinese Spring; STD: Standard deviation; FBA: Fructose-bisphosphate aldolase; HSP: Heat-shock protein.

Declarations

Acknowledgments

Not applicable

Author contribution statement

JGZ and LC conducted the entire study and drafted this manuscript. JNY did phenotype measurement. HPT, YM, Jun M, and YTG did field work. QTJ, and YXL helped with data analysis. GYC, JRW, PFQ, and AH did QTL analysis and manuscript revision. YMW revised manuscript. YLZ discussed results and revised the manuscript. XJL guided the study and revised the manuscript. Jian M designed the experiments, guided the entire study, participated in data analysis, wrote and extensively revised this manuscript. All authors participated in the research and approved the final manuscript.

Funding

This work is supported by the National Natural Science Foundation of China (31970243 and 31971937), the International Science and Technology Cooperation and Exchanges Program of Science and Technology Department of Sichuan Province (2021YFH0083), the Applied Basic Research Programs of Science and Technology Department of Sichuan Province (2020YJ0140 and 2021YJ0503), and the Basic Research Project of Science and Technology Plan of Guizhou Province (ZK[2021] General 131). We thank the anonymous referees for reading and revising this manuscript.

Availability of data and materials

The data that support the findings of this study are available in 'figshare' with the identifiers data DOIs, including dataset 1 (the genotypes of AM RILs using the wheat 55K SNP array from Mo et al. [18], <https://doi.org/10.6084/m9.figshare.14391629.v1>), dataset 2 (the genetic map information in this study from Mo et al. [18], <https://doi.org/10.6084/m9.figshare.14391749.v1>), dataset 3 (data of KL and KW of AM RILs in six environments, <https://doi.org/10.6084/m9.figshare.14392841.v1>), and dataset 4 (the DNA-seq data of AM RILs, <https://doi.org/10.6084/m9.figshare.14444798.v2>). Remaining data generated or analyzed during this study are included in this published article and its Additional files.

Compliance with ethical standards

Ethics approval and consent to participate

The wheat accessions (Ailanmai, LM001, AS 2268 and PI 503554, PI 193877) materials used in the experiment were supplied by Triticeae Research Institute of Sichuan Agricultural University and The U.S. National Plant Germplasm System (NPGS), respectively. These plant materials are widely used all over the world and no permits are required for the collection of plant samples. The plant materials are maintained in accordance with the institutional guidelines of Triticeae Research Institute of Sichuan Agricultural University, China. Experimental research and field studies on plants, including the collection of plant material, complied with relevant institutional, national, and international guidelines and legislation. Furthermore, this article did not contain any studies with human participants or animals and did not involve any endangered or protected species. All experiments and data analyses were conducted in Sichuan. The seedlings of F_8 AM RILs for DNA-seq came from 2019 Chongzhou, Sichuan province in this study. All authors contributed to the study and approved the final version for submission. The manuscript has not been submitted to any other journal.

Consent for publication

Not applicable.

Conflict of interest

All authors declare that there is no conflict of interest.

Author information

¹State Key Laboratory of Crop Gene Exploration and Utilization in Southwest China, Triticeae Research Institute, Sichuan Agricultural University, Chengdu, 611130, China

²College of Agronomy and Biotechnology, China Agricultural University, Beijing 100193, China

³Biotechnology and Genetic Engineering Discipline, Khulna University, Khulna 9208, Bangladesh

References

1. Wang DW, Li F, Cao SH, Zhang KP. Genomic and functional genomics analyses of gluten proteins and prospect for simultaneous improvement of end-use and health-related traits in wheat. *Theor Appl Genet.* 2020;133(5):1521-1539.
2. Zhao YL, Yang X, Zhou GH, Zhang T. Engineering plant virus resistance: from RNA silencing to genome editing strategies. *Plant Biotechnol J.* 2020;18(2):328-336.
3. Fan XL, Cui F, Ji J, Zhang W, Zhao XQ, Liu JJ, et al. Dissection of pleiotropic QTL regions controlling wheat spike characteristics under different nitrogen treatments using traditional and conditional QTL mapping. *Front Plant Sci.* 2019;10:187.
4. Desiderio F, Zarei L, Licciardello S, Cheghamirza K, Farshadfar E, Virzi N, et al. Genomic regions from an Iranian landrace increase kernel size in durum wheat. *Front Plant Sci.* 2019;10:448.
5. Yan XF, Zhao L, Ren Y, Dong ZD, Cui DQ, Chen F. Genome-wide association study revealed that the *TaGW8* gene was associated with kernel size in Chinese bread wheat. *Sci Rep-UK.* 2019;9(1):2702-2702.
6. Li MX, Wang ZL, Liang ZY, Shen WN, Sun FL, Xi YJ, et al. Quantitative trait loci analysis for kernel-related characteristics in common wheat (*Triticum aestivum* L.). *Crop Sci.* 2015;55:1-9.
7. Prashant R, Kadoo N, Desale C, Kore P, Dhaliwal HS, Chhuneja P, et al. Kernel morphometric traits in hexaploid wheat (*Triticum aestivum* L.) are modulated by intricate QTL × QTL and genotype × environment interactions. *J Cereal Sci.* 2012;56(2):432-439.
8. Xin F, Zhu T, Wei SW, Han YC, Zhao Y, Zhang DZ, et al. QTL mapping of kernel traits and validation of a major QTL for kernel length-width ratio using SNP and bulked segregant analysis in wheat. *Sci Rep-UK.* 2020;10(1):1-12.
9. Cheng XJ, Xin MM, Xu RB, Chen ZY, Cai WL, Chai LL, et al. A single amino acid substitution in STKc_GSK3 kinase conferring semispherical grains and its implications for the origin of *Triticum sphaerococcum*. *Plant Cell.* 2020;32(4):923-934.
10. Chen Y, Yan Y, Wu TT, Zhang GL, Yin HR, Chen W, et al. Cloning of wheat *keto-acyl thiolase 2B* reveals a role of jasmonic acid in grain weight determination. *Nat Commun.* 2020;11(1):1-11.
11. Lin Y, Chen GD, Hu HY, Yang XL, Zhang ZL, Jiang XJ, et al. Phenotypic and genetic variation in phosphorus-deficiency-tolerance traits in Chinese wheat landraces. *BMC Plant Biol.* 2020;20(1):1-9.
12. Li XJ, Jiang XL, Chen XD, Song J, Ren CC, Xiao YJ, et al. Molecular cytogenetic identification of a novel wheat-Agropyron elongatum chromosome translocation line with powdery mildew resistance. *PLoS ONE.* 2017;12(9):e0184462.

13. Assaf D, Hale I, Batsheva B-Z, Moran N, Raz A. QTLs for uniform grain dimensions and germination selected during wheat domestication are co-located on chromosome 4B. *Theor Appl Genet.* 2016;129: 1303-1315.
14. Russo MA, Ficco DBM, Laido G, Marone D, Papa R, Blanco A, et al. A dense durum wheat × *T. dicoccum* linkage map based on SNP markers for the study of seed morphology. *Mol Breeding.* 2014;34(4):1579-1597.
15. Okamoto Y, Takumi S. Pleiotropic effects of the elongated glume gene *P1* on grain and spikelet shape-related traits in tetraploid wheat. *Euphytica.* 2013;194(2):207-218.
16. Avni R, Oren L, Shabtay G, Assili S, Distelfeld A. Genome based meta-QTL analysis of grain weight in tetraploid wheat identifies rare alleles of *GRF4* associated with larger grains. *Genes.* 2018;9(12):636.
17. Zhou Y, Zhao XB, Li YW, Xu J, Bi AY, Kang LP, et al. *Triticum* population sequencing provides insights into wheat adaptation. *Nat Genet.* 2020;52(12):1412-1422.
18. Mo ZQ, Zhu J, Wei JT, Zhou JG, Xu Q, Tang HP, et al. The wheat 55K SNP-based exploration of loci for spikelet number per spike from a tetraploid wheat (*Triticum turgidum* L.) recombinant inbred line population derived from a Chinese landrace 'Ailanmai' and a wild emmer accession. *bioRxiv.* 2020;DOI:10.1101/2020.10.21.348227.
19. Liu YX, Lin Y, Gao S, Li ZY, Ma J, Deng M, et al. A genome-wide association study of 23 agronomic traits in Chinese wheat landraces. *Plant J.* 2017;91(5):861-873.
20. Gao YT, Xu XR, Jin JJ, Duan SN, Zhen WC, Xie CJ, et al. Dissecting the genetic basis of grain morphology traits in Chinese wheat by genome wide association study. *Euphytica.* 2021;217(4):56.
21. Ma J, Zhang H, Li SQ, Zou Y, Li T, Liu JJ, et al. Identification of quantitative trait loci for kernel traits in a wheat cultivar Chuannong16. *BMC Genetic.* 2019;20(1):77.
22. Lu P, Qin JX, Wang GX, Wang LL, Wang ZZ, Wu QH, et al. Comparative fine mapping of the *Wax 1 (W1)* locus in hexaploid wheat. *Theor Appl Genet.* 2015;128(8):1595-1603.
23. Smith SE, Kuehl R, Ray I, Hui R, Soleri D. Evaluation of simple methods for estimating broad-sense heritability in stands of randomly planted genotypes. *Crop Sci.* 1998;38(5):1125-1129.
24. Churchill GA, Doerge RW. Empirical threshold values for quantitative trait mapping. *Genetics.* 1994;138(3):963-971.
25. Ma J, Ding PY, Liu JJ, Li T, Zou YY, Habib A, et al. Identification and validation of a major and stably expressed QTL for spikelet number per spike in bread wheat. *Theor Appl Genet.* 2019;132(11):3155-3167.
26. Liu JJ, Luo W, Qin NN, Ding PY, Zhang H, Yang CC, et al. A 55 K SNP array-based genetic map and its utilization in QTL mapping for productive tiller number in common wheat. *Theor Appl Genet.* 2018;131(11):2439-2450.
27. Avni R, Nave M, Barad O, Baruch K, Twardziok SO, Gundlach H, et al. Wild emmer genome architecture and diversity elucidate wheat evolution and domestication. *Science.* 2017;357(6346):93-97.
28. IWGSC. Shifting the limits in wheat research and breeding using a fully annotated reference genome. *Science.* 2018;361:7193.
29. Ammiraju J, Dholakia B, Santra D, Singh H, Lagu M, Tamhankar S, et al. Identification of inter simple sequence repeat (ISSR) markers associated with seed size in wheat. *Theor Appl Genet.* 2001;102(5):726-732.
30. Ma J, Min S, Puyang D, Wei L, Xiaohong Z, Congcong Y, et al. Genetic identification of QTL for neck length of spike in wheat. *J Triticeae Crop (in Chinese).* 2017;3:319-324.
31. Yang T, Guo TC, Luo Y, Sun JH. Relationship between the anatomical structure and the grain formation of winter wheat varieties with different grain types. *Acta Agron Sinica (in Chinese).* 1998;24(6):876-883.
32. Liu KY, Xu H, Liu G, Guan PF, Zhou XY, Peng HR, et al. QTL mapping of flag leaf-related traits in wheat (*Triticum aestivum* L.). *Theor Appl Genet.* 2018;131(4):839-849.
33. Zhang GZ. Construction of high density genetic map and QTL analysis for yield, spike and grain size traits in wheat. *J Shandong Agr Univ (in Chinese).* 2014.

34. Tyagi S, Mir RR, Balyan HS, Gupta PK. Interval mapping and meta-QTL analysis of grain traits in common wheat (*Triticum aestivum* L.). *Euphytica*. 2015;201(3):367-380.
35. Kumar A, Mantovani EE, Seetan R, Soltani A, M ES. Dissection of genetic factors underlying wheat kernel shape and size in an elite x nonadapted cross using a high density SNP linkage map). *Plant Genome-US*. 2016;9(1):1-22.
36. Chen WG, Sun DZ, Yan X, Li RZ, Jing RL. QTL analysis of wheat kernel traits, and genetic effects of *qKW-6A* on kernel width. *Euphytica*. 2019;215:2-11.
37. Ramya P, Chaubal A, Kulkarni K, Gupta L, Kadoo N, Dhaliwal HS, et al. QTL mapping of 1000-kernel weight, kernel length, and kernel width in bread wheat (*Triticum aestivum* L.). *J Appl Genet*. 2010;51(4):421-429.
38. Li QF, Zhang Y, Liu TT, Wang FF, Liu K, Chen JS, et al. Genetic analysis of kernel weight and kernel size in wheat (*Triticum aestivum* L.) using unconditional and conditional QTL mapping. *Mol Breeding*. 2015;35(10):194.
39. Cui F, Fan XL, Chen M, Zhang N, Zhao CH, Zhang W, et al. QTL detection for wheat kernel size and quality and the responses of these traits to low nitrogen stress. *Theor Appl Genet*. 2016;129(3):469-484.
40. Cui F, Ding AM, Li J, Zhao CH, Li XF, Feng DS, et al. Wheat kernel dimensions: how do they contribute to kernel weight at an individual QTL level? *J Genet*. 2011;90(3):409-425.
41. Martin W, Mustafa AZ, Schnarrenberger HC. Higher-plant chloroplast and cytosolic fructose-1,6-bisphosphatase isoenzymes: origins via duplication rather than prokaryote-eukaryote divergence. *Plant Mol Biol*. 1996;32:485-491.
42. Plaxton WC. The organization and regulation of plant glycolysis. *Plant Mol Biol*. 1996;47(47):185-214.
43. Chen JF, Gao T, Wan SQ, Zhang YH, Yang JK, Yu YB, et al. Genome-wide identification, classification and expression analysis of the *HSP* gene superfamily in tea plant (*Camellia sinensis*). *Int J Mol Sci*. 2018;19(9):2633.
44. Prakash P, Sharma-Natu P, Ghildiyal MC. High temperature effect on starch synthase activity in relation to grain growth in wheat cultivars. *Indian J Plant Physiol*. 2003;8:390-398.
45. Iba K. Acclimative response to temperature stress in higher plants: approaches of gene engineering for temperature tolerance. *Annu Rev Plant Biol*. 2002;53:225-245.
46. Fan X, Cui F, Zhao C, Zhang W, Yang L, Zhao X, et al. QTLs for flag leaf size and their influence on yield-related traits in wheat (*Triticum aestivum* L.). *Mol Breeding*. 2015;35.

Figures

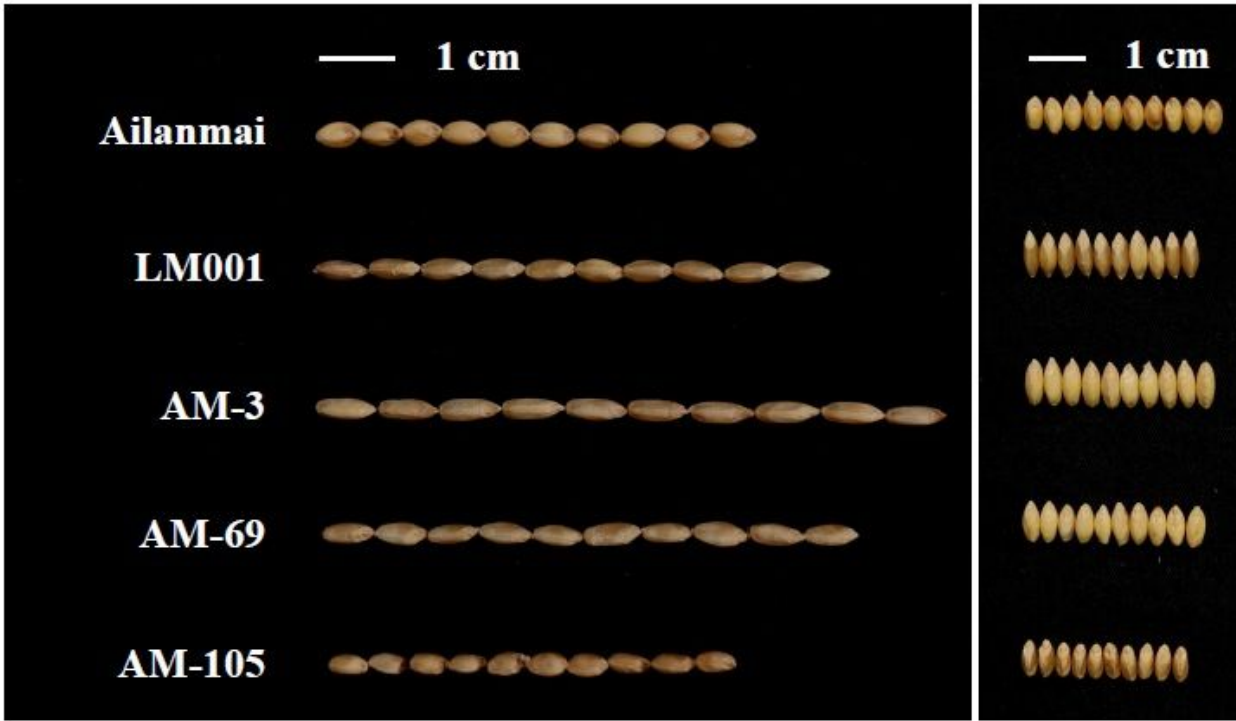


Figure 1

Phenotypes of the parents Ailanmai, LM001 and partial RILs. Comparison of kernel length and width among parents Ailanmai, LM001 and partial RIL (i.e. AM-3, AM-69 and AM-105). The white bar represents the scale = 1 cm.

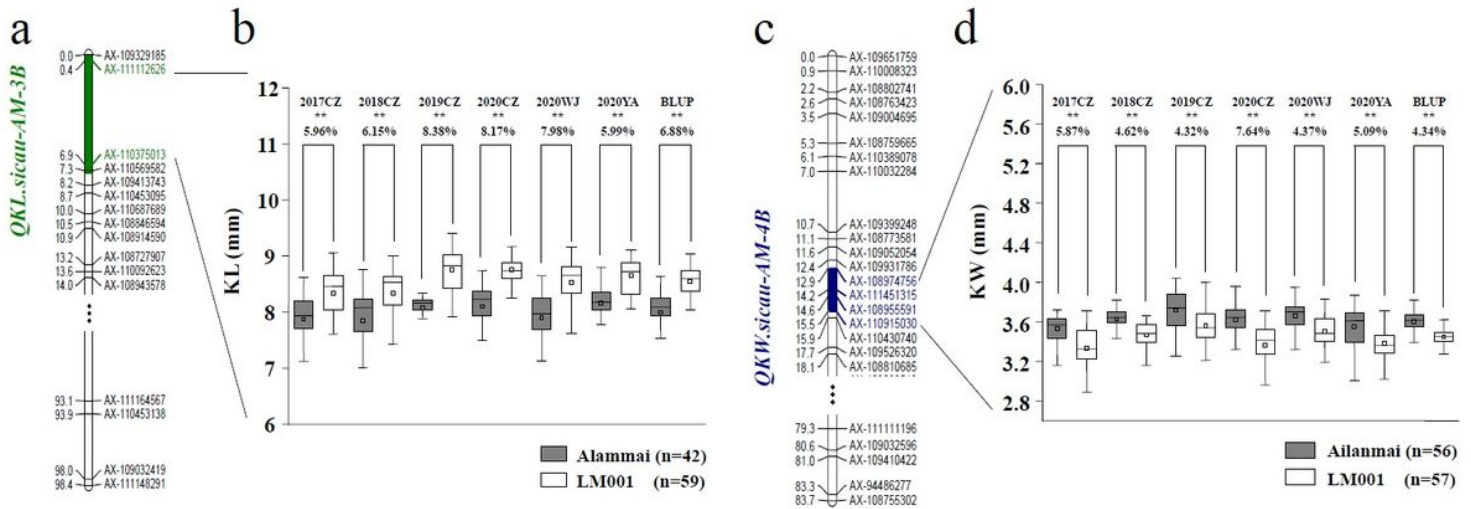


Figure 2

Major QTL *QKL.sicau-AM-3B* and *QKW.sicau-AM-4B* and their effects. (a): Genetic map of chromosome 3B; the green area was the interval of *QKL.sicau-AM-3B*; (b): effect of *QKL.sicau-AM-3B* shown as box plots calculated after grouping the AM population into two classes based on the flanking markers. Ailanmai and LM001 indicate the lines with and without positive alleles of *QKL.sicau-AM-3B*; (c): genetic map of chromosome 4B; The blue area was the interval of *QKW.sicau-AM-4B*; (d): effect of *QKW.sicau-AM-4B* shown as box plots calculated after grouping the AM population into two classes based on the flanking markers. CZ: Chongzhou; WJ: Wenjiang; YA: Ya'an; ** significance at the 0.01 probability level, *

significance at the 0.05 probability level. Differences between the two groups were labeled below the environmental names and BLUP.

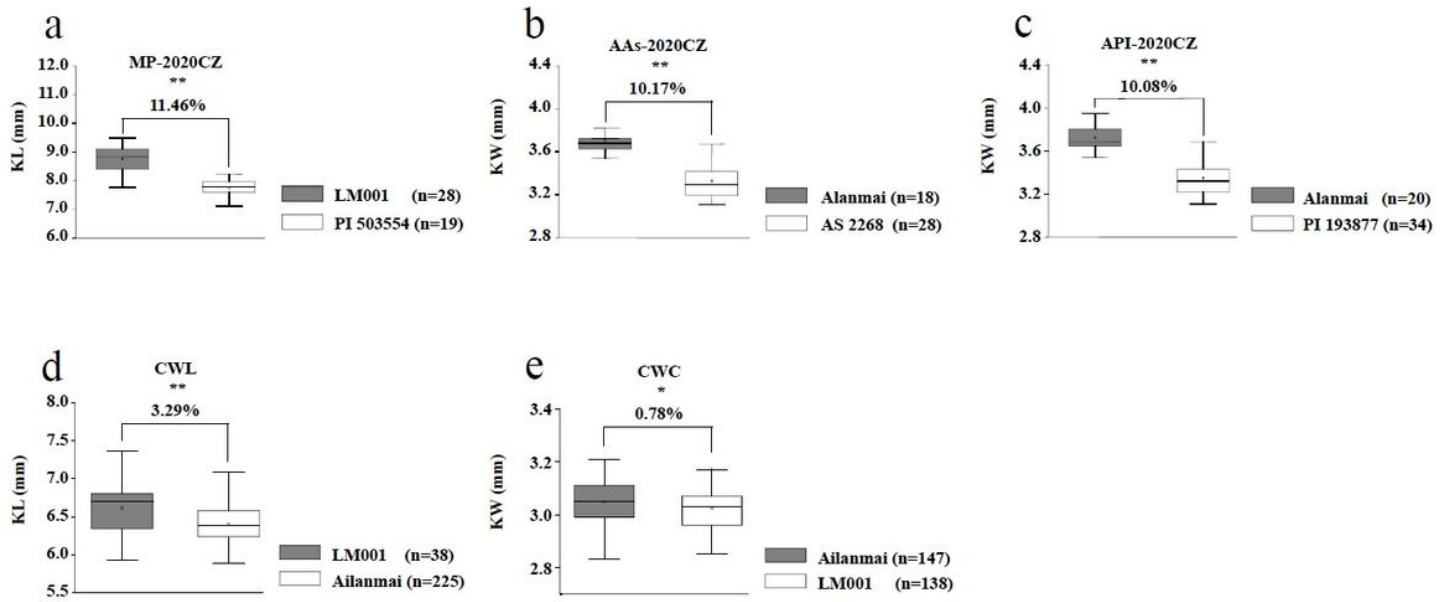


Figure 3

Verification of QKL.sicau-AM-3B and QKW.sicau-AM-4B in two and three different genetic background populations, respectively. (a), (d): Effects of QKL.sicau-AM-3B in the MP and the CWL validation populations, respectively; (b), (c), and (e): effects of QKW.sicau-AM-4B in the three populations (i.e. AAs, API and CWC). CZ: Chongzhou; ** significance at the 0.01 probability level, * significance at the 0.05 probability level.

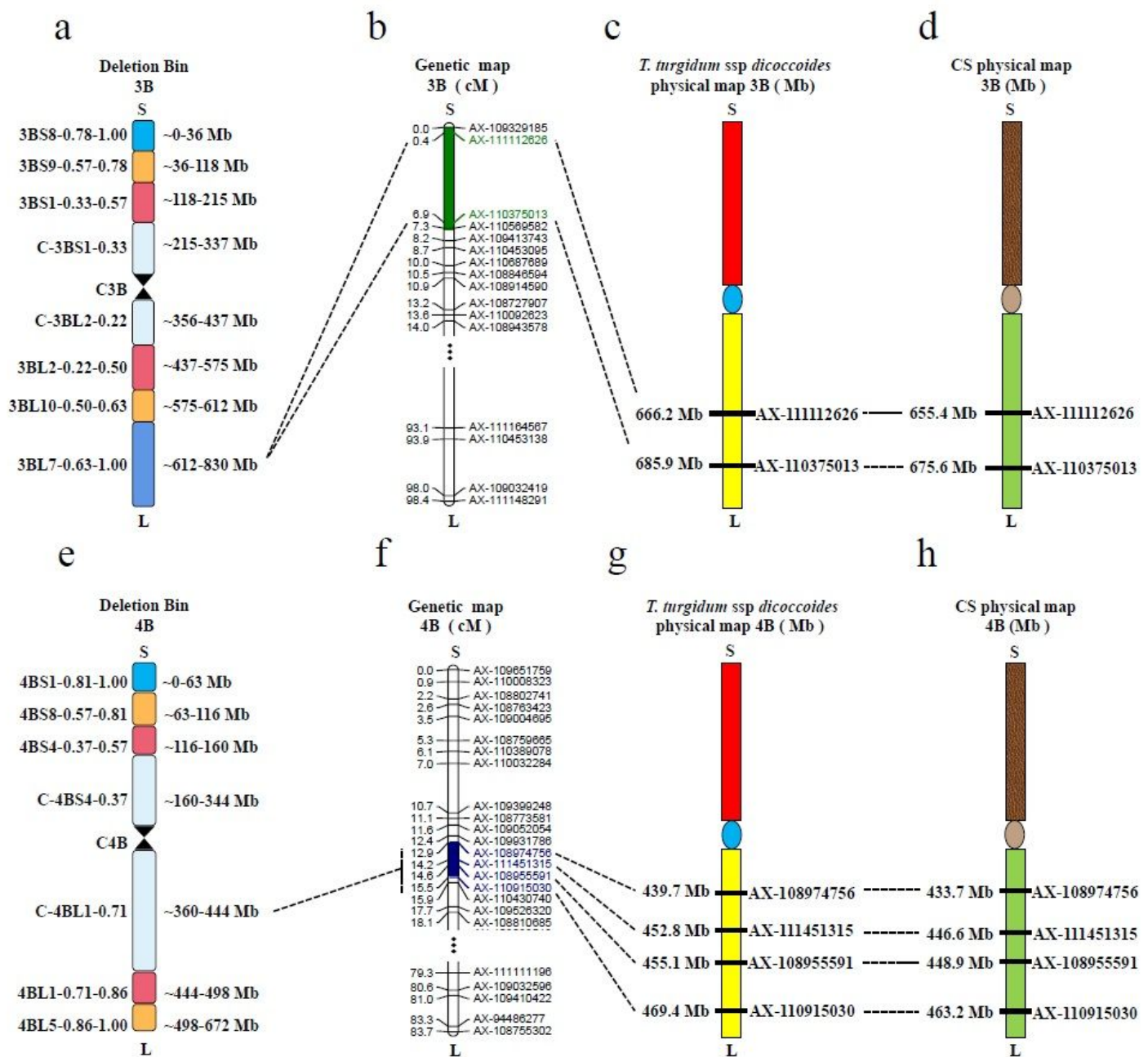


Figure 4

The physical interval of QKL.sicau-AM-3B and QKW.sicau-AM-4B. (a): Deletion bin map of wild emmer chromosome 3B; (b) partial genetic map of wheat chromosome 3B; (c): physical map of *T. turgidum* ssp. *dicoccoides* chromosome 3B; (d): physical map of CS chromosome 3B; (e): deletion bin map of wild emmer chromosome 4B; (f): partial genetic map of wheat (*Triticum aestivum* L.) chromosome 4B; (g): physical map of the wild emmer chromosome 4B; (h): physical map of CS chromosome 4B. The green and blue areas are the intervals of QKL.sicau-AM-3B and QKW.sicau-AM-4B, respectively, and the central area is centromere.

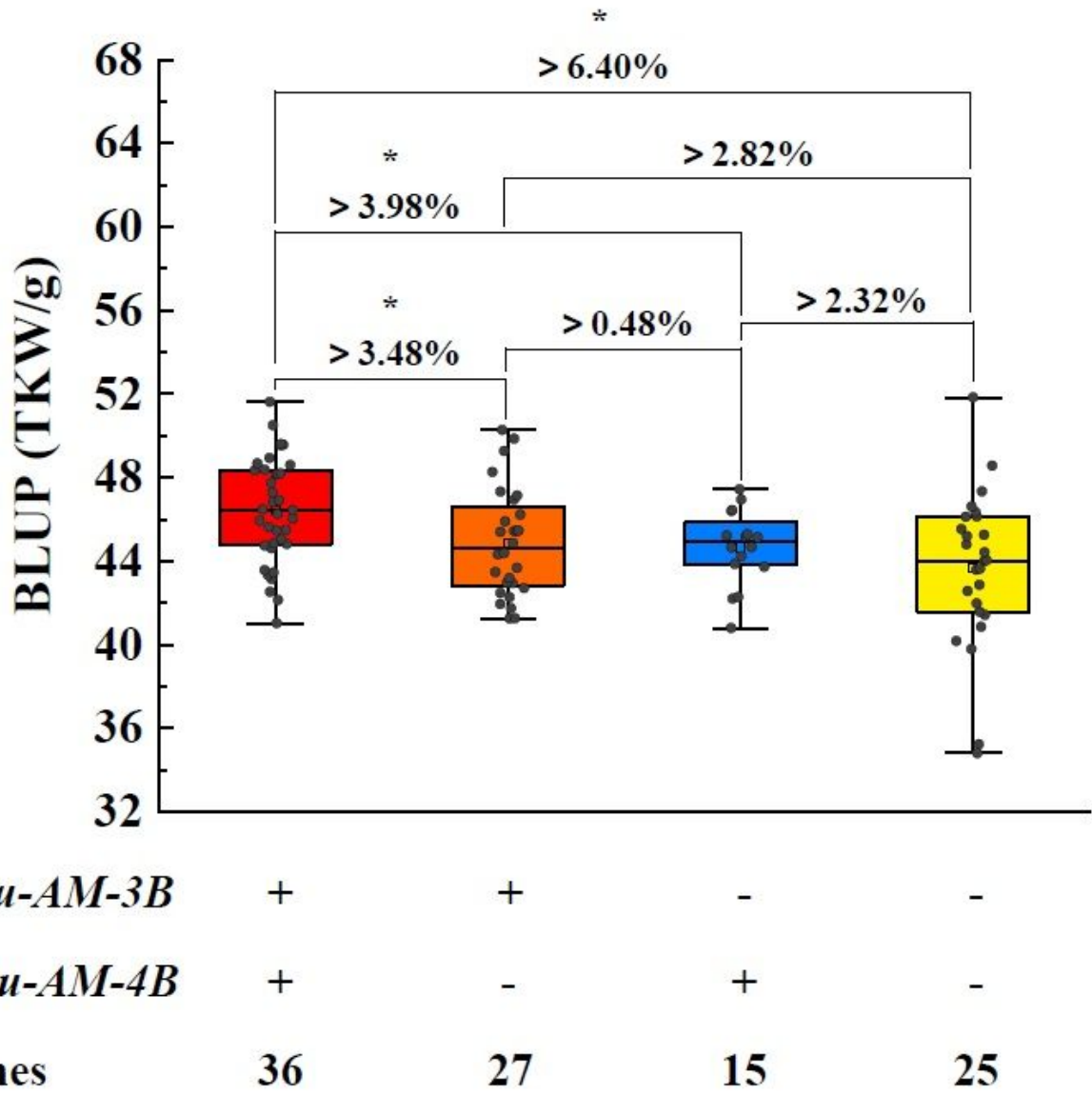


Figure 5

The effects of different combinations of *QKL.sicau-AM-3B* and *QKW.sicau-AM-4B* on increasing 1000-kernel weight (TKW) in the AM population. '+' and '-' represent lines with and without the positive allele of the corresponding QTL based on the genotype of flanking markers, respectively. * Significance at the 0.05 probability level.

Supplementary Files

This is a list of supplementary files associated with this preprint. Click to download.

- [Additionalfile1.xlsx](#)
- [Additionalfile2.xlsx](#)
- [Additionalfile3.xlsx](#)
- [Additionalfile4.pdf](#)

- [Additionalfile5.pdf](#)
- [Additionalfile6.xlsx](#)
- [Additionalfile7.xlsx](#)
- [Additionalfile8.xlsx](#)
- [Additionalfile9.pdf](#)
- [Additionalfile10.pdf](#)
- [Supplementaryinformationdescription.docx](#)